High-resolution Imaging of Catalytic Activity at a Single Graphene Sheet using Electrochemiluminescence Microscopy

Hui Zhu, Dechen Jiang,* Jun-Jie Zhu,*

State Key Laboratory of Analytical Chemistry for Life Science, School of Chemistry and Chemical Engineering, Nanjing University, Nanjing, Jiangsu, 210093, China

Corresponding authors: dechenjiang@nju.edu.cn (D.J); jjzhu@nju.edu.cn (J.Z).

Supporting Figures

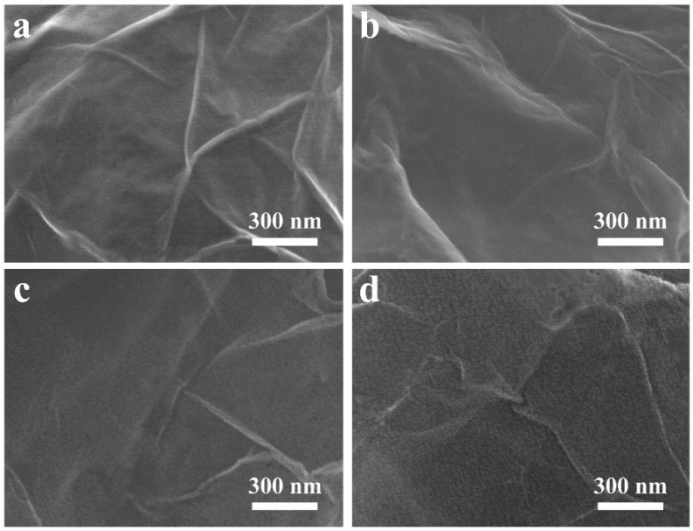

Supplementary Figure 1. SEM images of rGO microsheets after the O_2 plasma treatment for 0, 60, 120, 180s. A damage of morphology, as exhibited with a significantly increased roughness, is observed with an irradiation time over 120 s.

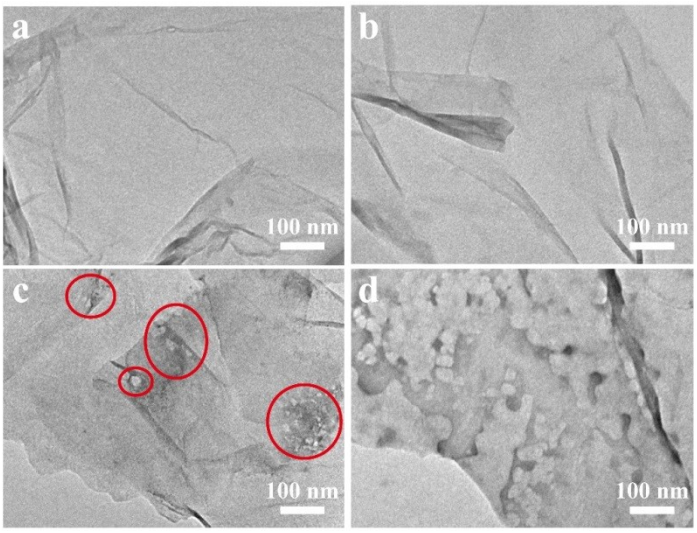

Supplementary Figure 2. TEM images of rGO microsheets after the O_2 plasma treatment for 0, 60, 120, 180 s. No obvious topographical change at the surface of rGO after the irradiation for 60 s. However, after the irradiation time exceeds 120 s, holes are generated (circled in red) and become bigger with an extended etching time.

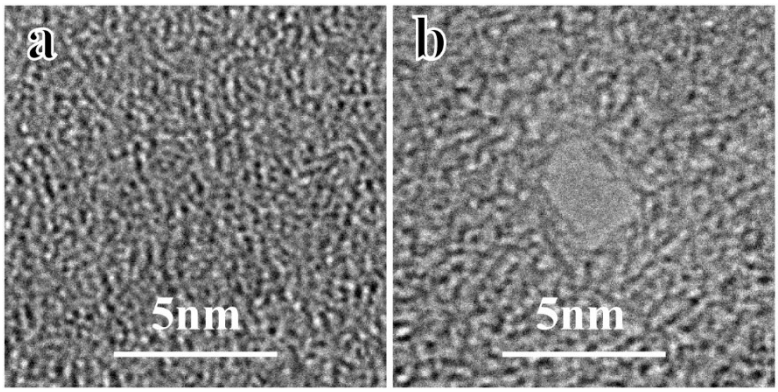

Supplementary Figure 3. The HRTEM of rGO (a) and rGO after the plasma treatment for 60 s (b). The HRTEM shows the hole with a diameter of ~ 3 nm indicating the formation of edge defects.

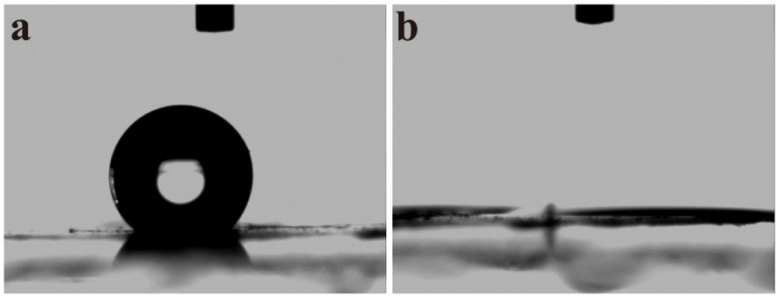

Supplementary Figure 4. The contact angle measurement of rGO (a) and rGO after the plasma treatment for 60 s (b). The contact angle measurement confirms that the treated rGO has a good electrolyte affinity and an increased specific surface area.

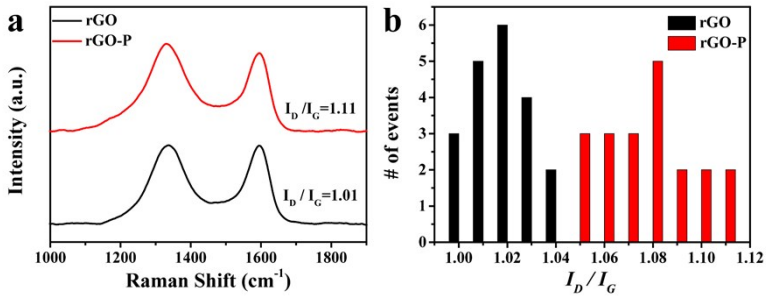

Supplementary Figure 5. (a) Raman characterization of rGO and rGO after plasma treatment (rGO-P) for 60 s; (b) the events of relative I_D/I_G intensity extracted from 20 individual rGO and rGO-P microsheets. The value of I_D/I_G from rGO-P is higher than that from rGO, confirming the formation of more defects at rGO after the plasma treatment.

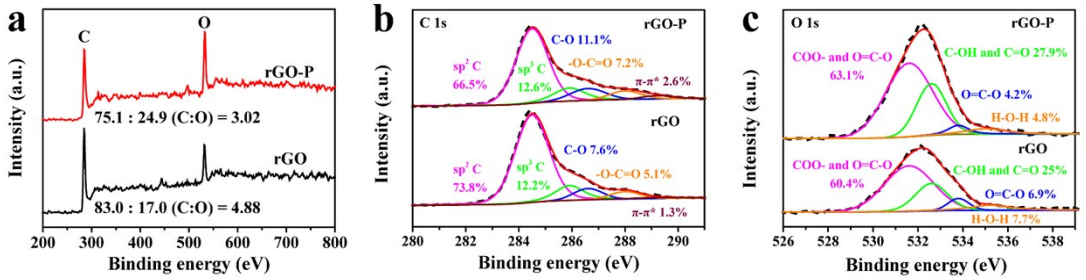

Supplementary Figure 6. (a) XPS of rGO and rGO after plasma treatment (rGO-P) for 60 s; (b) High resolution of C1s (b) and O1s (c). Compared with that at rGO, the O1s peak intensity in rGO-P is much higher (Figure S6a). The C/O (atom) ratio in rGO-P (3.02) is lower than that in rGO (4.88), demonstrating oxygen atoms are successfully introduced into rGO. In addition, C1s peaks in XPS spectrum are deconvoluted into the following five contributions: sp^2 carbon at 284.5eV (carbon in graphite); sp^3 carbon at 285.3eV (defects); epoxide/ether group(C-O) at 286.6 eV; carbonyl group(C=O) at 288.0 eV and carboxyl group(O=C-O) at 289.2 eV. After plasma treatment, only the value of sp^2 decreases significantly, while the other contributions increase. The ratio of sp^2/sp^3 decreases from 6.05 (rGO) to 5.28 (rGO-P), indicating more defects and edges at rGO-P. The O1s peak (Figure S6c) in the XPS spectra could be splited into four peaks at 531.6, 532.6, 533.8 and 535.2 eV, which are attributed to carboxyl group (COO-) in carboxylate and the oxygen double bond to carbon (O=C-O), hydroxyl (C-OH) and carbonyl (C=O), oxygen single bond in esters and carboxylic acids (O=C-O), chemisorbed oxygen or water (H-O-H), respectively. The decrease in the absorbed water or oxygen is attributed to the O_2 plasma treatment that removes surface adsorbed substances. The increase contents in COO-, O=C-O, C-OH and C=O indicate that more oxygenated functional groups are generated. Above all, edges and oxygenated functional groups are formed on rGO through O_2 plasma irradiation.

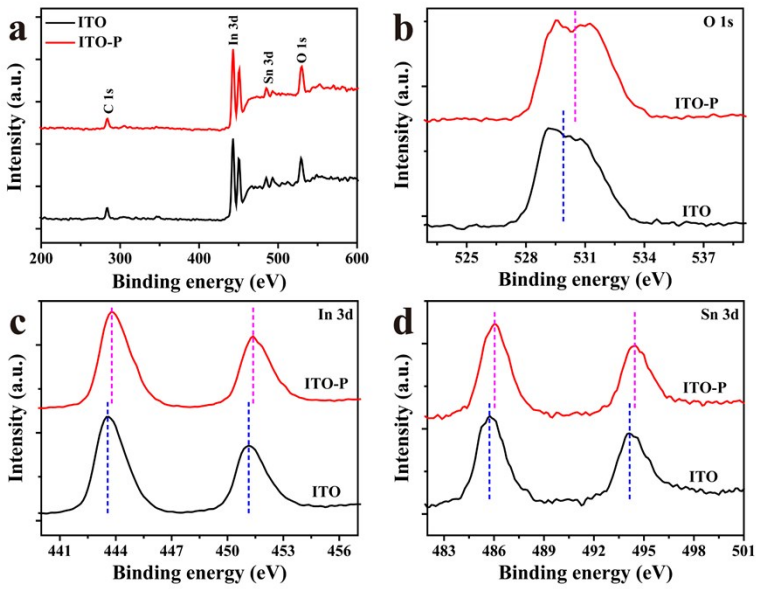

Supplementary Figure 7. (a) XPS of ITO and ITO after the oxygen plasma treatment (ITO-P) for 60 s; (b) high resolution of O1s, In3d and Sn3d of ITO and ITO-P. Due to the insertion of oxygen (Figure S7b), the binding energies of In3d and Sn3d increase (Figure S7c and d). This result shows that O_2 plasma introduces more oxygen at ITO surface, which is combined with In and Sn reducing the concentration of oxygen vacancies.

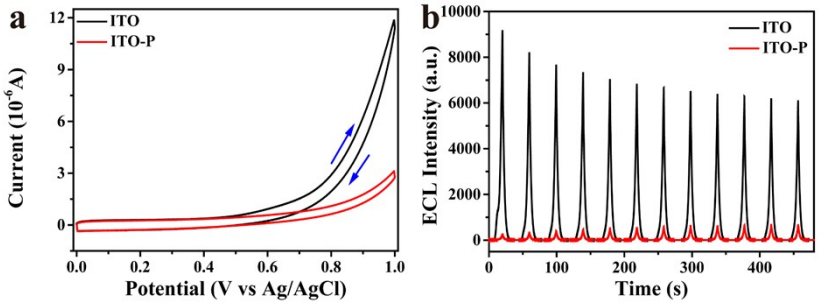

Supplementary Figure 8. Cyclic voltammetry (CV) curve (a) and the corresponding ECL curve (b) from ITO and ITO-P in 10 mM PBS solution (pH 10.0) containing 200 μM L012 and 1 mM H_2O_2. The voltage of PMT is set at 200 V. At the potential of 1.0 V, the current from ITO-P decreases by 4 times, and the corresponding ECL intensity decreases by more than 20 times.

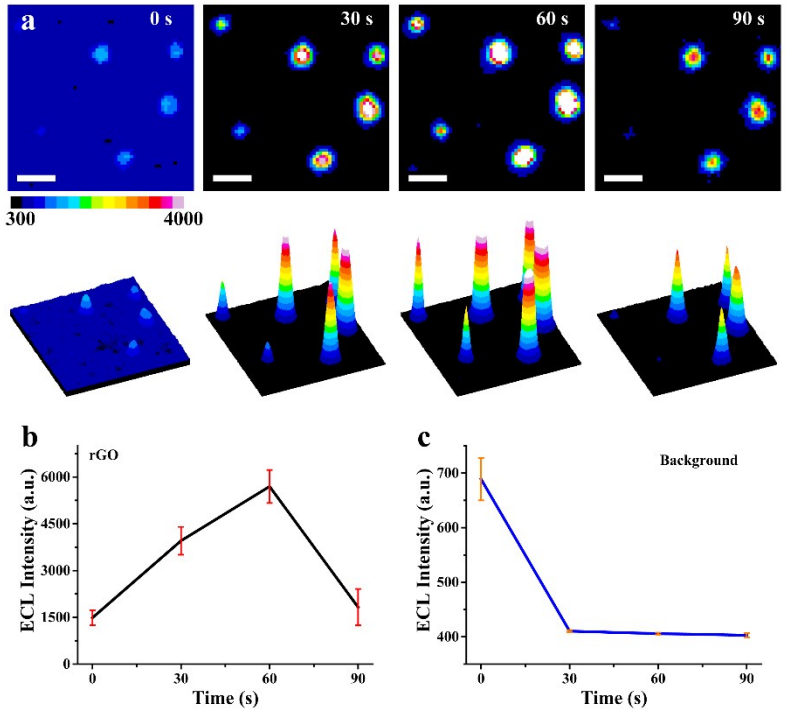

Supplementary Figure 9. (a) 2D and 3D ECL images of rGO microsheets after the plasma treatment for 0, 30, 60 and 90 s. (b) Statistical ECL intensity at rGO-P and (c) ITO surface after the plasma treatment. Scale bar: 10 μm. With the exposure time of 100 ms, the intrinsic noise intensity is ~ 400 a.u. At the treatment time of 0, 30, 60 and 90 s, the net background signals (the background signal subtracts the intrinsic signal) from ITO surface are 288, 10, 5 and 2 a.u., respectively, demonstrating the drop of the background intensity by at least 50 times.

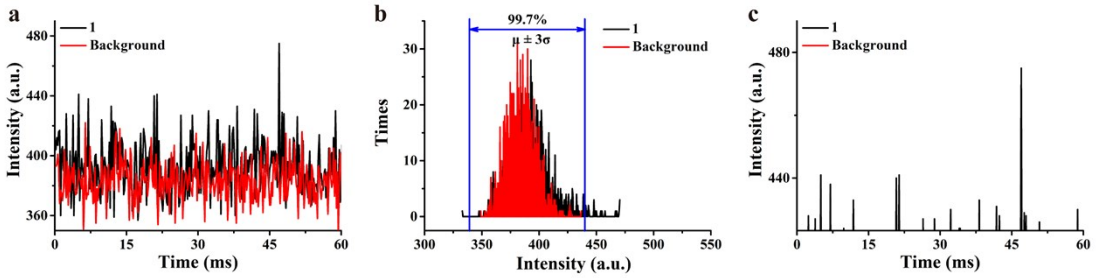

Supplementary Figure 10. (a) The ECL intensity of a pixel labeled '1' at rGO (black) and ITO slide (background) (red) with the exposure time of 0.2 ms. (b). Statistical distribution of data. The average value of background noise (μ) is 382.8 a.u. and the standard deviation (σ) is 13.5 a.u.. (c) The intermitted emission after the removal of noise. After excluding 3σ (99.7% of the background data within the range), no ECL burst observed in the background, while there are many ECL burst on rGO.

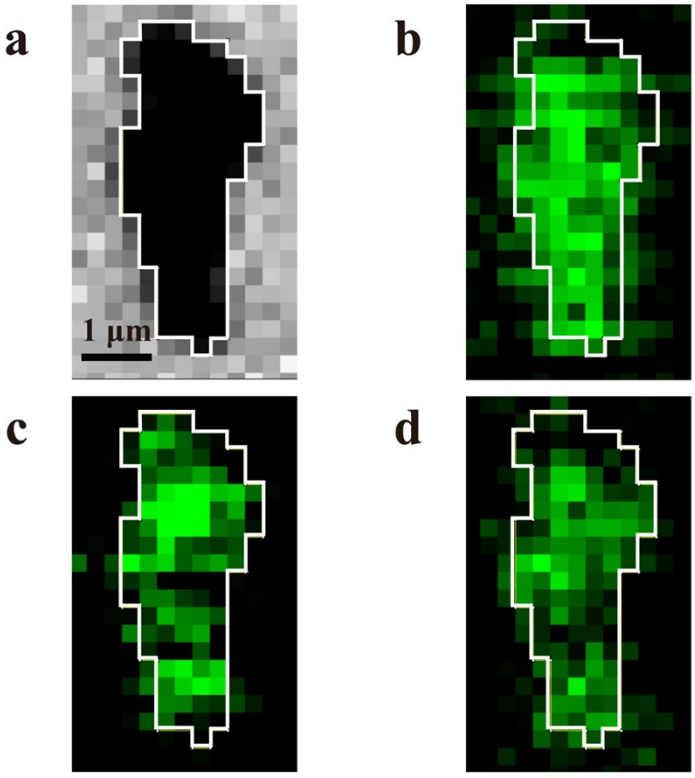

Supplementary Figure 11. (a) The bright-field image and (b-d) three stacked graphs from single rGO microsheets.